Advances in
Bridge Engineering

ORIGINAL INNOVATION Open Access

Research and application of rapid reconstruction technology to existing bridge guardrails based on UHPC connection

Yinggen Li[1], Zhiyong Li[1], Zheng Luo[2*] and Nan Yu[1]

*Correspondence:
13006@nbt.edu.cn

[1] Ningbo Communications Planning Institute Co., Ltd, Ningbo 315100, People's Republic of China
[2] School of Civil Engineering and Architecture, NingboTech University, Ningbo 315100, People's Republic of China

Abstract

A novel prefabricated segmental guardrail is proposed to facilitate connections between guardrails and between guardrails and bridge decks by casting ultrahigh-performance concrete (UHPC) joints in situ. Through finite element crash simulation analysis of three types of vehicles and crash tests of real vehicles, the prefabricated segmental guardrail with a UHPC connection was systematically evaluated in terms of its energy-absorbing capacity, vehicular acceleration, post-impact trajectory of the impacting vehicle, and behaviour of the guardrail upon impact. During the evaluation process, performance comparisons of the prefabricated segmental guardrails are made with the monolithic concrete guardrails. The results indicate that the performance of the prefabricated segmental guardrail with a UHPC connection was superior to that of the conventional concrete monolithic guardrails: it exhibited a higher level of crash performance, the occupants of the impacting vehicle were better protected, and the impacting vehicle exhibited better post-collision stability. Finally, the convenience of the prefabricated segmental guardrails with UHPC connections was proven in practical engineering applications.

Keywords: UHPC connection, Segmented prefabricated guardrails, Rapid construction, Finite element simulation, Crash tests of real vehicles

Reinforced concrete guardrails are important parts of highways and traffic safety facilities in municipal engineering because they block, buffer, and guide crashed vehicles to protect passengers safely, which is of great significance for driving safety. Recently, bridge guardrails have been subjected to frequent vehicular damage (Yang et al. 2019). The maintenance method of removing diseased guardrail and casting new guardrail on site has shortcomings, such as a long maintenance time during field operation, a wide range of lane closures, and prominent driving safety hazards during lane closures (Jeon and Choi 2011). Therefore, there is an urgent need for a rapid reconstruction method for existing bridge guardrails. Prefabricated section-assembled guardrails adopt factory prefabrication and on-site installation, which can solve several drawbacks of traditional cast-in-place guardrails (Namy et al. 2015). However, there are difficulties in the connection between the prefabricated guardrail and the bridge deck, and the longitudinal

connection between the segmented prefabricated guardrails (Khodayari et al. 2023; Namy et al. 2015).

The method for connecting bridge decks and prefabricated guardrails must be simple while ensuring adequate safety under vehicle impact and effective load transmission between components. Thus, numerous research initiatives have been focused on creating creative prefabricated guardrail system connections. To investigate the failure patterns of various guardrail configurations, Patel et al. (2014) experimentally built a guardrail–deck connection using post-tensioned threaded steel rods. Basit et al. (2020) created a prefabricated concrete guardrail system using spliced loop reinforcement and grouted mortar to improve the integrity of a guardrail–bridge deck connection. Ultra-high-performance concrete (UHPC) (Bandelt et al. 2023; Fan et al. 2023; Charron et al. 2011) has been used recently in prefabricated component connections, new building construction, and structural restorations and renovations. Although UHPC has gained increasing interest, it has not been widely used owing to its high cost (Fan et al. 2022; Hung et al. 2021). Nonetheless, using UHPC as a connecting material can be the most economical option. The binding strength of UHPC is approximately eight times greater than that of normal concrete based on a previous assessment of UHPC anchorage performance (Shao et al. 2022). UHPC can significantly increase the reinforcement anchoring strength, and hence reduce the required lap length when used as an in-situ grout in the connections between structural elements (Sohail et al. 2021). Thus, this study created a prefabricated segmental guardrail with UHPC connections between individual guardrail segments and the deck.

Therefore, this study used UHPC as the key connection material for section-assembled anticrash concrete guardrails, which contributed to its excellent crash resistance, satisfying the assembly requirements of anticrash guardrails. Through finite element simulation, crash test of real vehicles, and practical engineering applications, we verified the blocking, buffering, and guiding functions of the segmented prefabricated guardrails connected by UHPC, as well as the reliability of the key connection parts of UHPC and the operability of practical applications.

1 Rapid reconstruction method for existing bridge guardrails based on UHPC connection

Rapid reconstruction technology for existing bridge guardrails based on UHPC connection (hereinafter referred to as "rapid reconstruction method for UHPC-connected guardrails") is a rapid reconstruction method for existing bridge guardrails. It used UHPC as the connection material for prefabricated segmented guardrails and bridge decks and the longitudinal connection material for prefabricated segmented guardrails. The length of each segmented prefabricated guardrail was four metres (the curved segments could be two meters long). The segmented guardrails were prefabricated in a factory, transported to the site for installation after maintenance, and reached the design strength. The key connection parts were then poured into the UHPC.

Each prefabricated segmented guardrail was provided with a UHPC pouring hole with a diameter of 10 cm and a longitudinal spacing of 100 cm. It was used to pour the UHPC inward to connect the guardrails and bridge decks. An epoxy resin adhesive was used to fill the gaps between the reserved slots of the prefabricated segmented guardrails, and

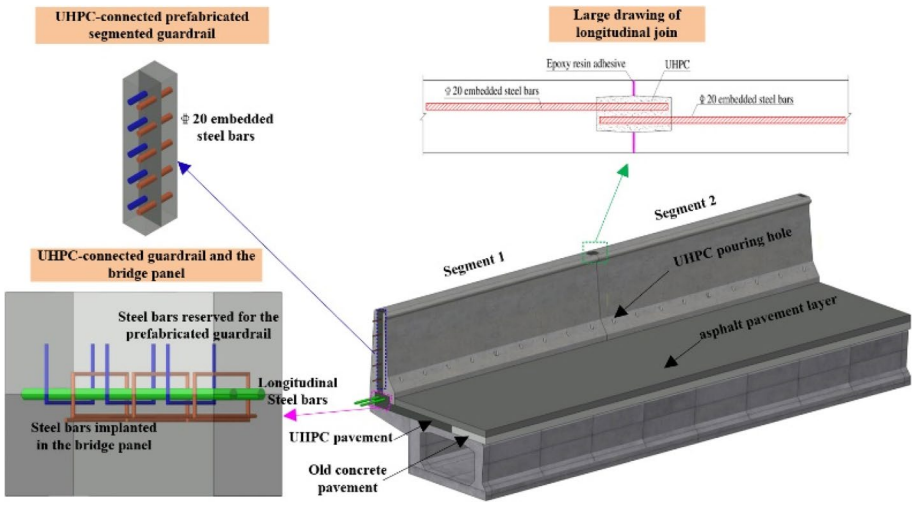

Fig. 1 Guardrail reconstruction structure

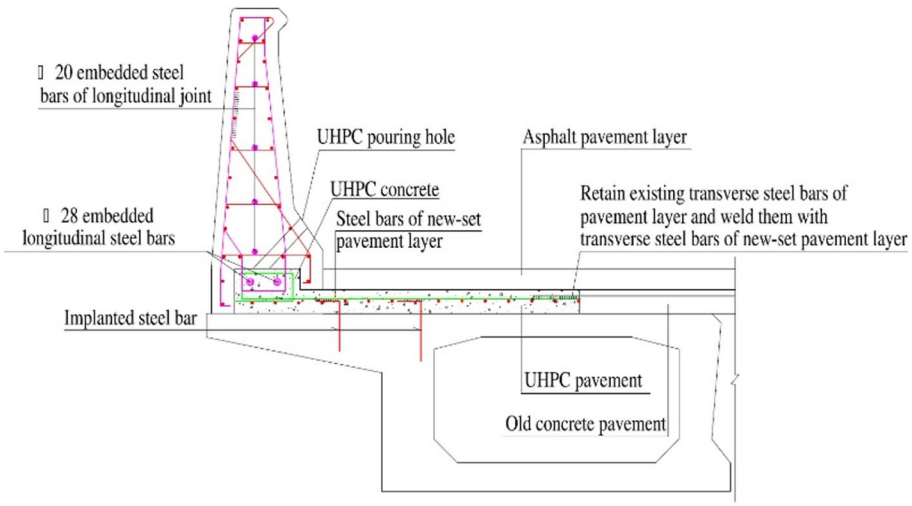

Fig. 2 Guardrail reconstruction rebar reinforcement

then UHPC was injected to connect each prefabricated segmented guardrail. Additionally, there were five embedded steel bars with a diameter of 20 mm and a transverse staggered arrangement on each side of the prefabricated segmented guardrail. The steel bars of the paving layer, implanted in the bridge deck and reserved for the prefabricated guardrail, were connected using two longitudinal steel bars with a diameter of 28 mm. The main structure and rebar are shown in Figs. 1 and 2.

Rapid reconstruction method for UHPC-connected guardrails has the following advantages (Bandelt et al. 2023; Fan et al. 2023; Fan et al. 2022):

(1) Full use of the ultrahigh bond strength between UHPC and steel bars. The use of UHPC grouting material can significantly shorten the anchoring length of the steel bars and improve the coordination ability of the steel bars and concrete in the post-casting area.

Table 1 Vehicle types and crash parameters

Vehicle types	Total weight (tonne)	Crash velocity (km/h)	Crash angle (°)
Car	1.5	100	20
Bus	14	80	20
Truck	25	60	20

Table 2 Vehicle basic parameters

Vehicle types	Total weight (tonne)	Length (m)	Width (m)	Mass centre height (m)
Car	1.5	4.6	1.8	0.518
Bus	14	11	2.5	1.29
Truck	25	12	2.4	1.581

(2) The UHPC cast-in layer is set in the negative bending-moment area of the cantilever plate of the bridge floor, giving full play to the characteristics of UHPC high-strength material, effectively solving the pain point that the anti-crash ability of the guardrail is increasing but the cantilever plate of the bridge floor needs to be strengthened in the past reconstruction projects, as well as increasing the safety margin of the structure.

(3) The guardrail reconstruction method for factory prefabrication and on-site installation significantly reduces the field operation time, lane sealing time, and field operation space and is particularly suitable for emergency guardrail reconstruction projects.

This study will verify the blocking, cushioning, and guiding performance of UHPC-connected prefabricated segmental guardrail as well as the reliability of critical connecting joints through finite element analysis and actual vehicle crash tests.

2 Finite element analysis

2.1 Finite element model

2.1.1 Vehicle model

The vehicle types and crash parameters based on the requirements of the "Standard for Safety Performance Evaluation of Highway Guardrail" (JTGB05-01-2013, n.d.) are listed in Tables 1 and 2. In the simulation analysis of each vehicle crashing into a segmented prefabricated guardrail, a group of normal monolithic concrete guardrails was used as the control group.

Using the LS-DYNA finite element software, the cars adopted common cars on the highway. To reduce the calculation time, the car model was simplified, interior decorations such as the seats and steering wheel inside the car were deleted, and equal mass points were used to replace them. The engine model was established using a No. 20 rigid unit. A large number of shell units were used throughout the car to establish its shape. Hourglassing can be kept in check by invoking a suitable Hourglass control algorithm that creates internal forces to resist hourglass modes (LSTC 2014). The hourglass used

for global control adopts No.5 hourglass calculation formula based on stiffness and its coefficient is set to 0.05. The buses adopted the same simplified method as the cars, and the trucks adopted the semi-tractor established by the USA National Crash Analysis Center (NCAC), which is composed of a tractor and truck. The primary vehicle models are shown in Fig. 3.

2.1.2 Guardrail model

The concrete guardrails were simulated using the reduced integration of eight-node solid elements. The material behaviour of concrete in this model was depicted using the continuous surface cap model (CSCM) (Murray and Evone 2007), which can capture crucial aspects of inelastic concrete behaviour, such as post-peak softening and confinement effects. However, the CSCM, which is typically calibrated for normal concrete with a compressive strength of 28–58 MPa, is not suitable for modelling UHPC used in connections, which has a significantly higher material strength of ~ 152 MPa. To overcome this issue, a modified version of the CSCM was incorporated into our analysis to simulate the unique response characteristics of UHPC. The steel rebars were represented by beam elements using an elastic–plastic (MAT 24) material model. This study adopted the dynamic increase factor (DIF) of the concrete and steel rebars for the compressive and tensile strengths proposed by Hao. The accuracy of this model in simulating the performance of concrete structures under impact loading has been validated in several studies. In addition, a perfect bond between the rebars and surrounding concrete was assumed in the model using the keyword CONSTRAINED_LAGRANGE_IN_ SOLID. After a mesh convergence test, an optimum mesh size of 20 mm was utilised for the solid and beam elements to balance accuracy and efficiency.

The guardrail model and related boundary conditions were established based on the design drawings. The guardrail and floor deck were connected by UHPC in the crash of real vehicles, and the ground was considered as a rigid body, which restricted all degrees of freedom. A 40 m-long guardrail model was established according to the specifications, with each segment being 4 m long. Keyword *CONTACT_AUTO-MATIC_SURFACE_TO_SURFACE was used between segmented prefabricated guardrails. The contact stiffness was set as 1.0. A common node was adopted between the UHPC and ordinary concrete in the prefabricated segmented guardrails, and automatic surface contact was adopted between the ground, UHPC, and guardrails. Keyword *CONSTRAINED_LAGRANGE_IN_SOLID was used between steel bar reinforcement and concrete, which used Lagrangian algorithm to simulate the bond and slip characteristics between steel bar reinforcement and concrete.

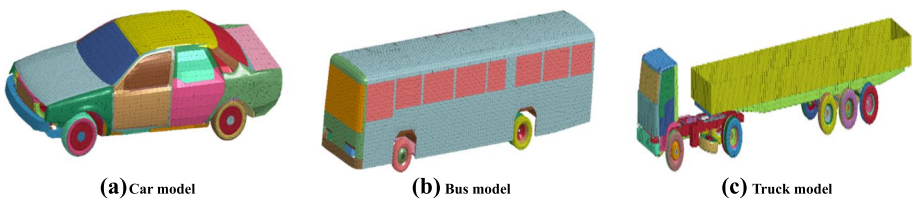

Fig. 3 Vehicle finite element model

We investigated the interface behaviour between UHPC and concrete in prefabricated members. We used the AUTOMATIC SURFACE TO SURFACE TIEBREAK (ASTS_T) algorithm in LS-DYNA to simulate various aspects of the bonding interface. This included modelling the bonding, cracking, and post-cracking slip while considering the initial bond caused by the adhesive effects and the subsequent frictional contact after the failure of the initial adhesive bond. The criterion for the bond failure at the connection interface was established as follows:

$$\frac{(|\sigma_n|)^2}{\mathrm{NFLS}} + \frac{(|\sigma_s|)^2}{\mathrm{SFLS}} \geqslant 1 \tag{1}$$

where NFLS and SFLS denote the interfacial normal tensile and shear strengths, respectively. In this study, we defined the interfacial tensile strength NFLS as the tensile strength of the concrete on both sides of the interface, which was 3.31 MPa. The shear strength, SFLS, was calculated using the following equation:

$$\mathrm{SFLS}=\tau_d=c_a \cdot f_t+\mu \cdot \sigma_n \tag{2}$$

where c_a is the coefficient for the adhesive bond and μ is the friction coefficient between concrete and UHPC; μ was used as an important parameter for the contact behaviour at the interface of prefabricated columns and was used to study the impact dynamic response of pocket columns or socketed columns, as shown in Sect. 4.2. In addition, previous studies employed a range of tests, including slant shear and splitting tensile tests, to evaluate the shear strength of the interface between UHPC and concrete. Researchers have concluded that the optimal values of cohesion c and friction coefficient μ for the UHPC-NC interface with a rough surface are 2.2 MPa and 1.37 (Fang et al. 2020), respectively. The boundary conditions for the prefabricated segmental guardrail model comprised simultaneous fixing of the bottom and inside faces of the bridge–deck overhang. To investigate the performance variations among different types of guardrails, this study also developed an number model for monolithic CIP concrete guardrails. A comparative analysis of the failure processes of the four models was subsequently conducted under identical loading conditions.

2.1.3 Model of vehicle guardrails

Based on the specifications, the crash point was set at the L/3 starting point of the standard section of the guardrail, where the guardrails were in contact. During collision simulations, the truck was placed on an infinite ground (*RIGIDWALL_PLANAR) with a frictional coefficient of 0.2, which was 0.5 m above the pier bottom corresponding to the buried depth of the footing. In particular, the contact between the heavy truck and bridge pier was realised by *CONTACT_ ERODING_SURFACE_TO_SURFACE with static and dynamic frictional coefficients of 0.4 and 0.3, respectively (Chen et al. 2018). The calculation time was 1.0 s. In addition, the X-axis of the vehicle driving direction was defined as the horizontal axis, whereas the Y-axis, vertical to the vehicle driving direction, was defined as the vertical axis. A finite element model of the vehicle-crashing guardrail is shown in Fig. 4 and 5. Only a model of the car-crashing guardrails is presented here. The models for other vehicles that crash on guardrails are similar.

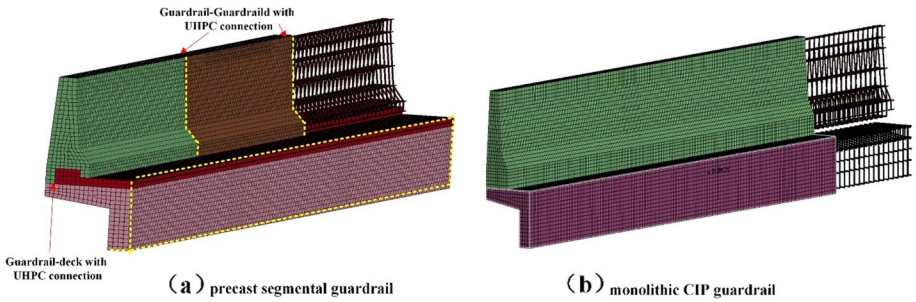

Fig. 4 Prefabricated segmental guardrail with UHPC connection model

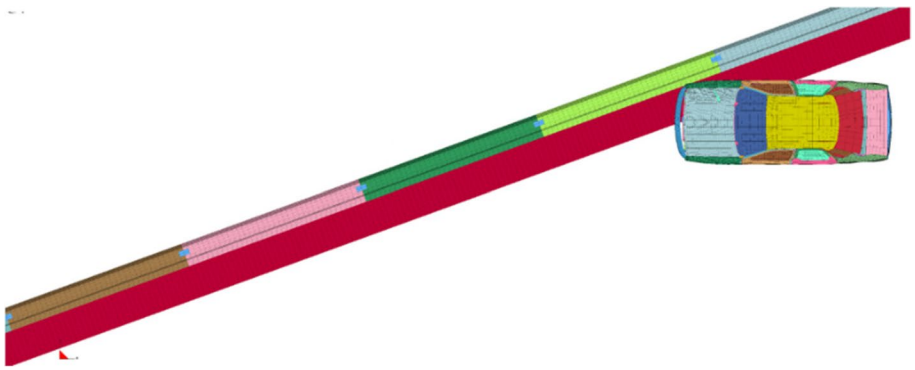

Fig. 5 Finite element model of the vehicle guardrails

2.2 Evaluation of blocking and guiding functions

2.2.1 Car

The post-processing software LS-DYNA was used to describe the crash process. During the entire process, the car did not ride, turn, or cross over the guardrail, and there was no intrusion of guardrail components into the interior of the car. Therefore, the prefabricated segmented guardrails were assumed to have an effective blocking performance (Liu et al. 2007).

The driving trajectory of the car during a crash is shown in Figs. 6 and 7. The measured driving-out angle of the car after the crash was 10°, which was less than the required 12°, based on the specifications. The entire crash process was divided into two stages: ① the front hits the guardrail in 0.1 s, then immediately, the direction of the vehicle becomes parallel to the guardrail; ② the rear of the car hits the guardrail in 0.2 s owing to inertia, making the direction of the vehicle deviate from the guardrail and causing the car to rush out of the road to the sky. It can be seen from the guide chart that the wheel track after the crash was in the exit frame. A segmented prefabricated guardrail can provide good guidance.

2.2.2 Bus

Because the heads of buses are high and their bodies are long, they can easily overturn when they crash into the guardrails, causing serious life hazards to occupants. Therefore, there are more stringent requirements for the blocking and guiding functions of prefabricated segmented guardrails. A bus with a weight of 14 t and speed of 80 km/h was

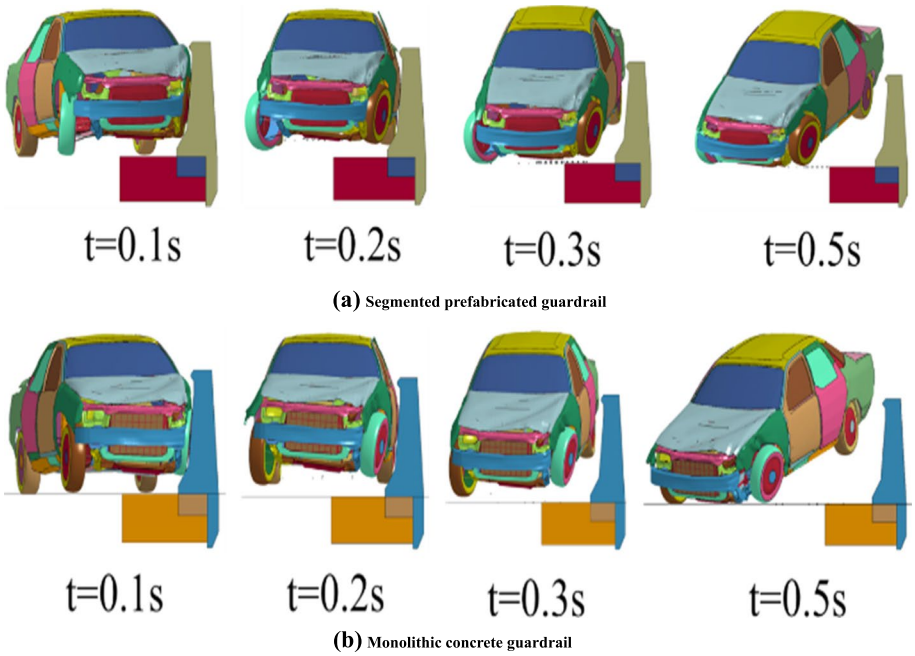

Fig. 6 Process of car crashing guardrail

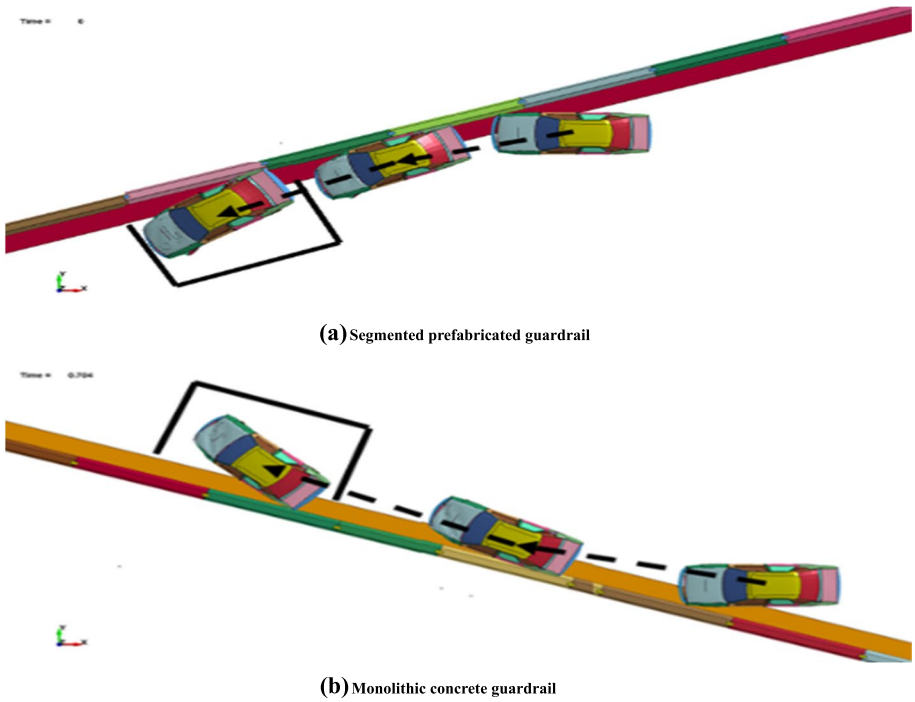

Fig. 7 Car driving trajectory during crash

selected for a 20° oblique crash to analyse and evaluate the safety of the prefabricated segmented guardrail.

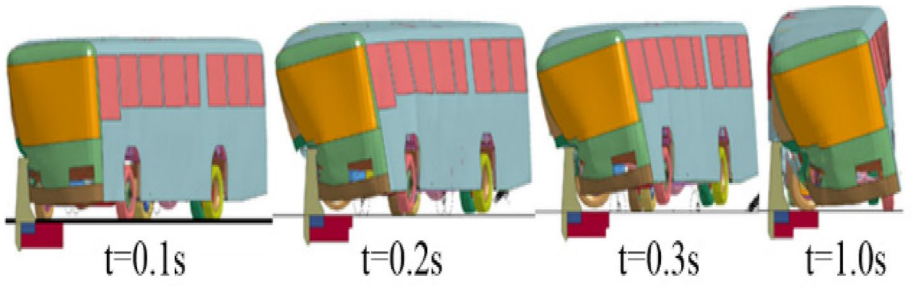

(a) Segmented prefabricated guardrail

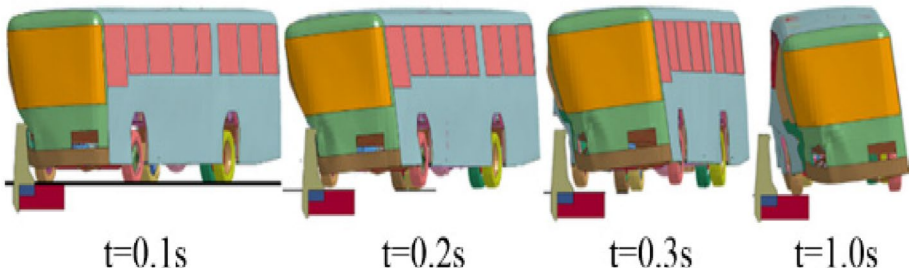

(b) Monolithic concrete guardrails

Fig. 8 Process of bus crashing guardrail

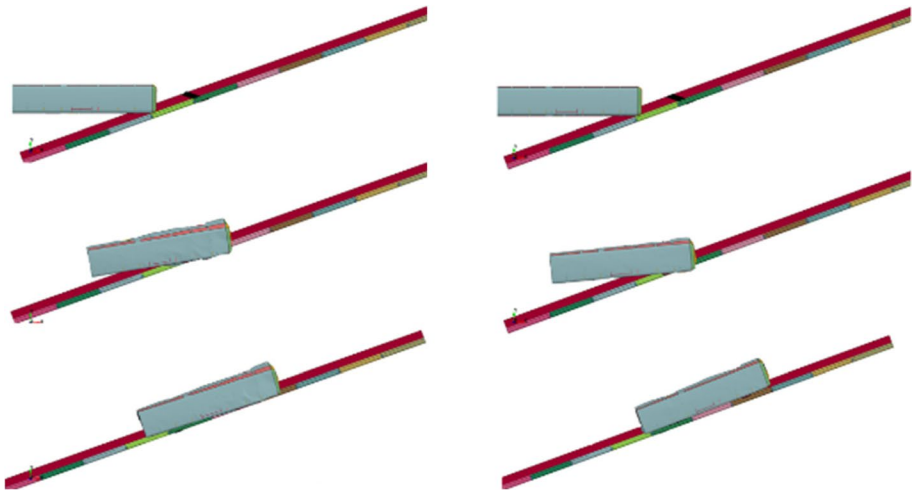

(a) Segmented prefabricated guardrail **(b)** Monolithic concrete guardrails

Fig. 9 Bus driving trajectory during crash

As shown in Fig. 8, the front of the bus crashed into the segmented prefabricated guardrail at 0.1 s, and the front of the bus was deformed until 0.3 s, during which time the bus front leaned on the guardrail and slipped for a certain distance. After 0.3 s, the bus gradually drifted toward the guardrail until the entire bus completely depends on the guardrail. As shown in Fig. 9, during the entire process, the entire bus did not ride, cross, or turn over the guardrail. In addition, after the crash, the bus ran along the direction

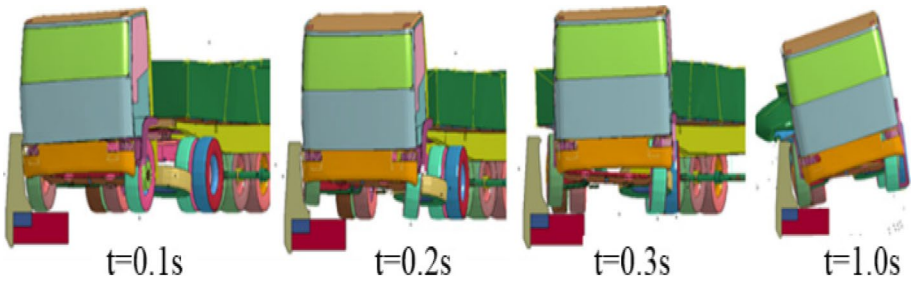

(a) Segmented Prefabricated Guardrail

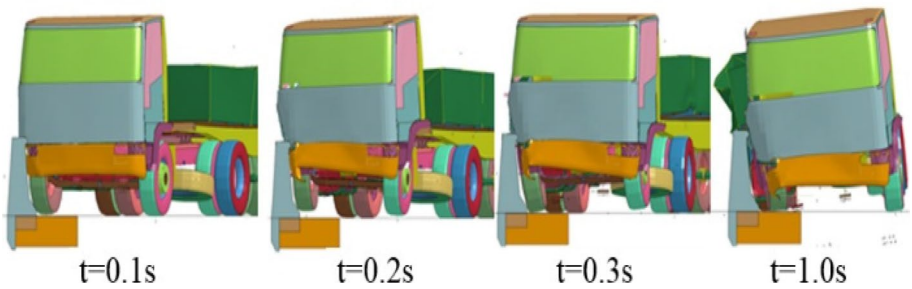

(b) Monolithic Concrete Guardrail

Fig. 10 Process of Truck Crashing Guardrail

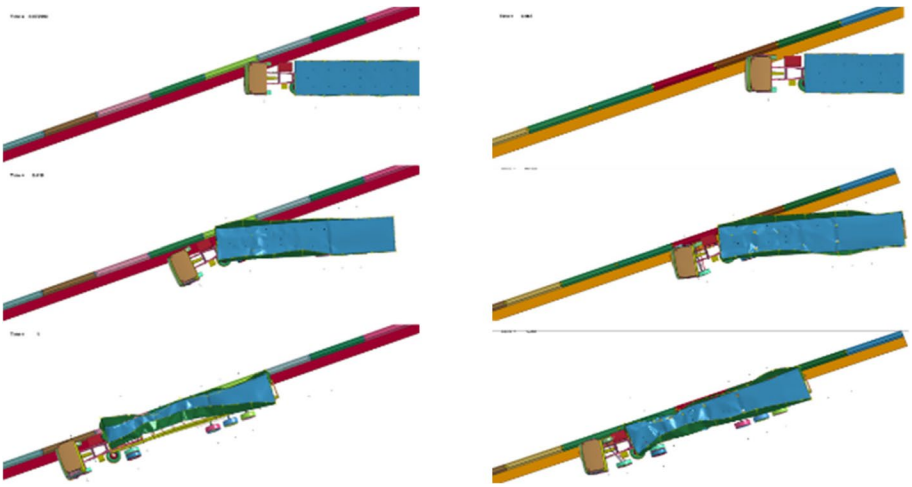

(a) Segmented Prefabricated Guardrail **(b)** Monolithic Concrete Guardrails

Fig. 11 Truck driving trajectory during crash

of the guardrail, which was less than 60% of the crash angle. This indicates that the segmented prefabricated guardrail has good blocking and guiding functions.

2.2.3 Truck

As shown in Figs. 10 and 11, when the truck crashed into the guardrail, it did not cross, climb, or ride over the guardrail. The front of the tractor hit the segmented prefabricated guardrail at 0.1 s and then changed its driving direction along the direction of the guardrail. It crashed into the guardrail by the body side owing to inertial drift at approximately

0.8 s, and finally maintained a certain tilt angle and leaned against the guardrail. The deformation of the truck front was more serious when it crashed into an ordinary concrete guardrail than into the segmented prefabricated guardrail. In summary, segmented prefabricated guardrails can effectively prevent trucks from careening off the road, while simultaneously providing good guidance.

2.3 Vehicle-guardrail dynamic response

In contrast to monolithic cast guardrails, prefabricated segmental guardrails consist of individual segments prefabricated off-site and joined together by UHPC during installation, where joints between segments can affect load transfer and structural integrity. The contact force generated by the crash between the vehicle and the guardrail can often reflect the crashing process, and the strength of the crash force can also reflect the buffer capacity of the guardrail.

2.3.1 Car

The collision forces between the car and the guardrail are shown in Fig. 12a. When the car hit the segmented guardrail and the monolithic cast-in-place guardrail, two peaks were generated at 0.08 and 0.18 s, respectively, corresponding to the aforementioned front and rear collisions. Compared with the time-course curves of the transverse collision force, the responses of the prefabricated segmented guardrail and the monolithic cast-in-place guardrail are basically the same. The collision force between the cart and the guardrail is shown in Fig. 12b. From the figure, it can be learned that the small car reaches a peak lateral acceleration of about 15 g at 0.05 and then rapidly reduces to 0. The rear end of the car hits the guardrail at 0.15 s, at which time the lateral acceleration peaks once again at about 10 g. The above peak acceleration is less than the specification of 20 g. In addition, the small car collision section prefabricated and assembled guardrail acceleration response time course and the overall cast-in-place guardrail after the vehicle's maximum acceleration are basically the same. Figure 12c analyzes and compares the dynamic lateral displacement and deformation values of the top of the guardrail at the point of impact when the car hits the prefabricated, assembled guardrail and the overall cast-in-place guardrail. From the figure, it can be seen that the guardrail is mainly deformed elastically under the impact speed of 100 km/h of the car, and the residual deformation value is very small after the end of the impact. Two peaks also appeared in the dynamic displacement curve corresponding to the front and rear impacts,

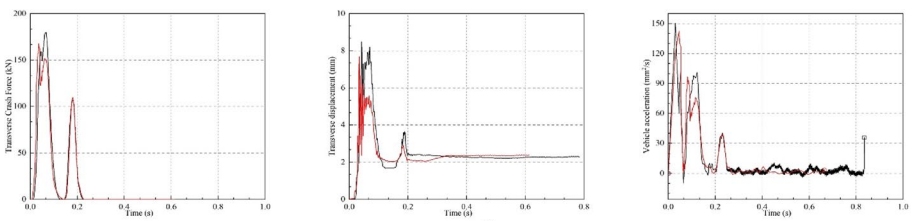

(a) Time-course curve of transverse crash force

(b) Time-course curve of transverse displacement

(c) Time-course curve of vehicle acceleration

Fig. 12 Car-guardrail dynamic response

respectively. Also, from the figure, we can know that the dynamic displacement value of the prefabricated segmental guardrail is lower than that of the cast-in-place guardrail.

2.3.2 Bus

Figure 13a gives a comparison of the impact force curves of the prefabricated segmental guardrail and the monolithic cast-in-place guardrail. It can be clearly seen that there are two obvious wave peaks when the large bus impacts the monolithic cast-in-place guardrail, corresponding to the front end and rear end impacts, respectively, and the second rear end impact produces an impact force that is much higher than that of the first front-end impact, with a value of about two times that of the first impact. The prefabricated segmental guardrail has only one wave peak in the whole process of bus impact, which coincides with the impact process reflected in Fig. 15a. Therefore, the prefabricated segmental guardrail has fewer impacts and is safer only from the impact force time-course curve. Vehicle acceleration time curve as shown in Fig. 13b, passenger car impact integral cast-in-place monolithic cast guardrail, there are two peaks, corresponding to the front impact and rear impact, respectively. In the rear impact integral cast-in-place guardrail, its acceleration component reached 45 g, which exceeded the specification of the requirements of 20 g. The acceleration trend of prefabricated, assembled guardrail is more gentle, and there is no obvious sudden change in the section. Therefore, prefabricated segmental guardrails have a better buffer effect, which can better ensure the safety of passengers. The maximum dynamic displacement of the guardrail is shown in Fig. 13c. The lateral displacement of the precast segmental guardrail is slightly larger than that of the whole cast-in-place guardrail, which is because the acceleration generated by the front end of the vehicle is larger; with the rear end of the vehicle hitting the guardrail, the displacement of the whole cast-in-place guardrail rises rapidly, and the magnitude of the displacement increase is higher than that of the front end of the vehicle hitting the front end of the vehicle, and the rear end of the large passenger car hitting the prefabricated assembly guardrail with a very small power response, so at this time the guardrail impact point has a better buffering effect, which can better guarantee the safety of passengers. Therefore, the displacement value at the impact point of the guardrail at this time does not exist in the in the fluctuation section; in general, prefabricated, assembled guardrails in the impact of large buses produce a smaller dynamic displacement value.

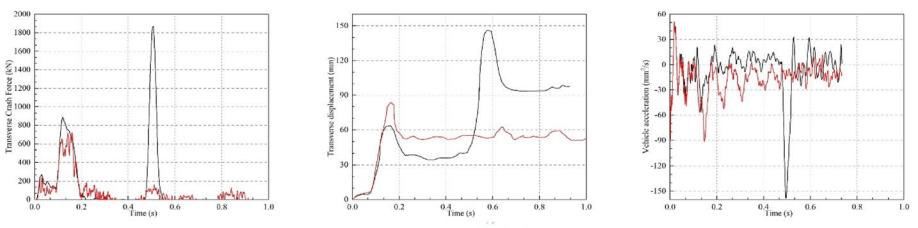

(a) Time-course curve of transverse crash force

(b) Time-course curve of transverse displacement

(c) Time-course curve of vehicle acceleration

Fig. 13 Bus-guardrail dynamic response

2.3.3 Truck

The time-course curve of the truck-guardrail impact force is shown in Fig. 14a. In the front-end impact, the peak lateral impact force of the segmental precast assembled guardrail is lower than that of the ordinary monolithic cast guardrail. From Fig. 14c, it can be seen that the dynamic displacement of the guardrail shows a step-like increasing trend; the displacement of the guardrail reaches the peak value in 0.2 s in the front impact and reaches the second peak value in the rear impact, and there is a small decrease after each displacement reaches the peak value, which is caused by the recovered elastic deformation. Since the truck body is long, except for the front end and the rear end of the trailer hitting the guardrail, the rest of the parts are not in contact with the guardrail, so there is a long and almost unchanged plateau section of the dynamic displacement time curve. Comparing the two types of guardrail, the segmental prefabricated assembled guardrail produces less displacement under truck impact. In addition, in the process of truck impact on the guardrail, the internal energy of the precast segmental guardrail is much smaller than that of the monolithic cast-in-place guardrail (Fig. 14d), and the damage to the precast segmental guardrail is therefore smaller than that of the monolithic cast-in-place guardrail, which demonstrates that the former has a good ability to dissipate the energy of vehicle impact.

In summary, the segmented prefabricated guardrails were consistent with the ordinary cast-in-place reinforced concrete guardrails and exhibited good blocking and guiding

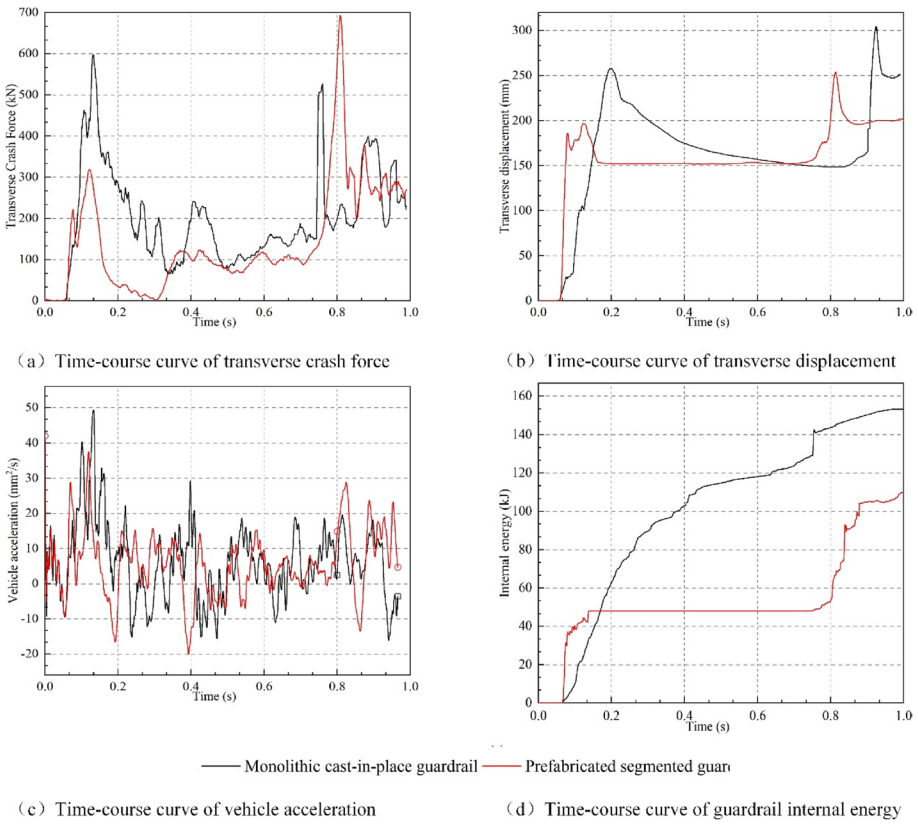

（a）Time-course curve of transverse crash force

（b）Time-course curve of transverse displacement

（c）Time-course curve of vehicle acceleration

（d）Time-course curve of guardrail internal energy

Fig. 14 Truck-guardrail dynamic response

Fig. 15 Crash test sites for real vehicles

Fig. 16 Real vehicles used in the crash test

performances. In addition, the prefabricated segmented guardrails exhibited better buffering and energy absorption effects.

3 Crash test on real vehicles

3.1 Crash conditions

A crash test was conducted on a full-scale real truck. The mass of the truck was 25 t, the crash speed was 60 km/h, the crash angle was 20°, and the crash energy reached 400 kJ. The steering system, suspension system, wheels, and loading conditions of the front and rear axles of the truck satisfied the requirements of the "Standard for Safety Performance Evaluation of Highway Guardrail" (JTG B05-01 2013). The crash test sites for the real vehicles are shown in Figs. 15 and 16.

3.2 Crash process analysis

The full course of the truck's impact on the prefabricated segmental guardrail is shown in Fig. 17. During the test, the truck was guided into the test setup by the remote steering system. The vehicle obliquely crashed into the joint of the prefabricated segmented

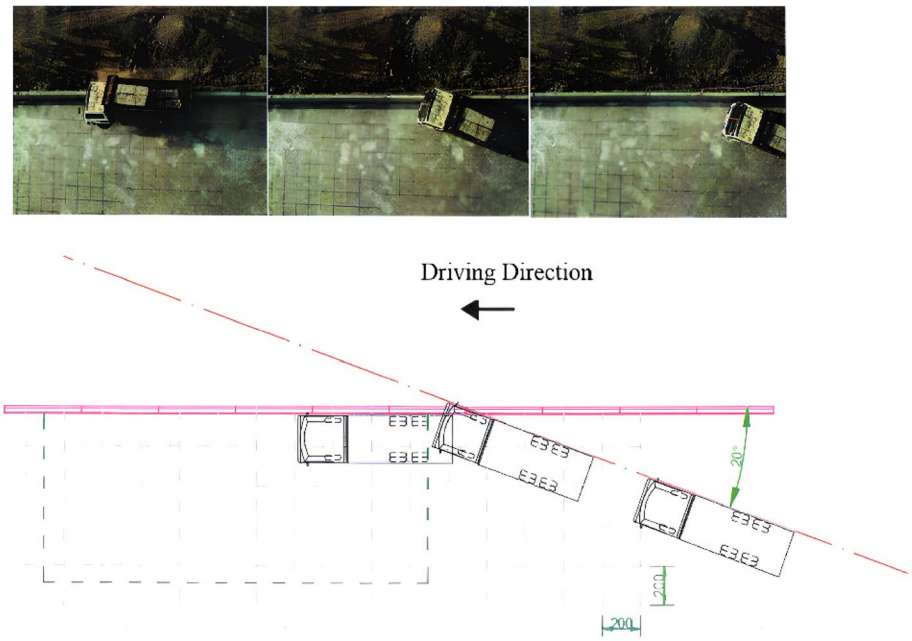

Fig. 17 Driving track line for real vehicle crash

guardrails at an angle of 20°. At 0.100 s, the cab of the test vehicle began to steer, and the lower right front corner of the van trailer came into contact with the top of the guardrail near the top of the guardrail at 0.203 s. The van trailer began to run parallel to the guardrail at 0.667 s. The lower right corner of the van trailer came into contact with the top of the guardrail near the top of the guardrail at 0.695 s and broke off near the top of the guardrail at 0.748 s. At 0.748 s, the right rear edge of the van trailer ruptured. As the test vehicle continued along the guardrail, it veered to the right off the end of the guardrail wall. The test vehicle's brakes failed to apply and the test vehicle then came to rest 35.66 m downstream of the end of the guardrail.

Evaluation criteria for full-scale vehicle crash testing are based on three appraisal areas, namely: (i) structural adequacy; (ii) occupant risk; and (iii) vehicle trajectory after collision. Structural adequacy is judged upon the ability of the guardrail to contain and redirect the vehicle, or bring the vehicle to a controlled stop in a predictable manner. The vehicle should not penetrate, underride, or override the guardrail. Occupant risk criteria evaluate the potential risk of hazard to occupants in the impacting vehicle and to some extend other traffic, pedestrian, or workers in construction zones, if applicable; deformation of, or intrusions into, the occupant compartment should not exceed pre-set limits set forth in specification; and whether the vehicle remain upright during and after collision. Post impact vehicle trajectory is assessed to determine potential for secondary impact with other vehicles or fixed objects, creating further risk of injury to occupants of the impacting vehicle and/or risk of injury to occupants in other vehicles. Crash test results showed that the guardrail contained and redirected the 36 tonnes truck. The vehicle did not penetrate, underride or override the parapet. No detached elements, fragments, or other debris from the guardrail were present to penetrate or show potential for penetrating the occupant compartment, or to present undue hazard to others

in the area. No occupant compartment deformation occurred. The 36 tonnes truck test remained upright during and after the collision event.

3.3 Analysis of crash results

The crash results are as follows:

(1) Overall, as shown in Fig. 18, only the concrete portion at the surface of the crash point was slightly broken; the other parts remained basically intact without significant damage, indicating that the prefabricated segmented guardrails could effectively absorb and disperse the crash energy during crash and transfer it to different segments.
(2) The UHPC joints between the guardrails and bases, and those between the segmented prefabricated guardrails exhibited good crashworthiness. The key UHPC joints were verified to be reliable. Furthermore, it proved the importance and superiority of UHPC joints in prefabricated segmented guardrails, which ensure the strength and stability of the joints, effectively prevent crash energy from concentrating on a single guardrail segment, and improve the overall crash resistance and durability.

The crash test on real vehicles further verified the reliability of the UHPC-connected prefabricated guardrails, strongly supporting the rapid reconstruction method for UHPC-connected guardrails.

4 Practical engineering application

A rapid reconstruction method for UHPC-connected guardrails was successfully applied to a highway emergency repair project in Ningbo. Owing to vehicle collisions and fires, the reinforced concrete guardrails on the southern connector of the Ningbo Hangzhou Bay Cross-Sea Bridge was severely damaged, as shown in Fig. 19. In addition, because current anticrash bridge guardrails can no longer satisfy the current standard collision prevention requirements, it is necessary to upgrade and reconstruct anticrash bridge guardrails (Gendron et al. 2022; Khodayari et al. 2023). Therefore, the rapid reconstruction method for UHPC-connected guardrails proposed in this study was applied to this project, as shown in Fig. 20.

The specific construction method for UHPC connection prefabricated segmental guardrails is outlined as follows:

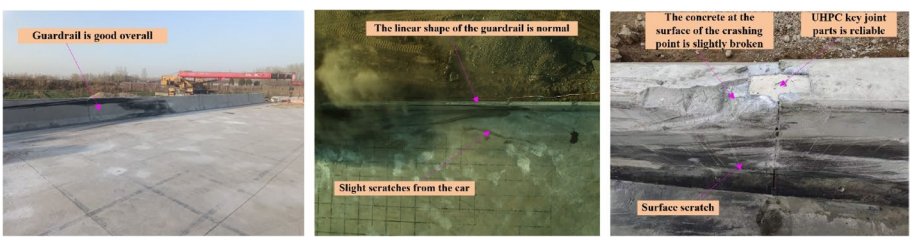

Fig. 18 Damage on segmented prefabricated guardrails

Fig. 19 Damage to existing bridge guardrails

Fig. 20 Main process of existing bridge guardrail reconstruction

(1) Perform prefabrication work such as reinforcement binding, pouring, and curing for the guardrail segments, as illustrated in Fig. 20a and b. During the prefabrication process of the guardrail segments, vertical connecting rebars are required to be reserved at the bottom of the segments for staggered anchoring with UHPC, while longitudinal connecting rebars are reserved on both sides of the segments.
(2) Remove the original damaged guardrail along with a certain range of asphalt and concrete pavement layers. However, during the removal process, it is necessary to retain the original transverse rebars in the pavement layers, as depicted in Fig. 20c. This is done to facilitate the connection of transverse rebars with the vertical connecting rebars of UHPC, ensuring a good transverse connection between UHPC vertical connections and pavement layers for overall lateral load transfer. After transporting the guardrail segments to the site, they are hoisted into position using a crane. The guardrail segments are then positioned and fixed, as depicted in Fig. 20d.
(3) Vertical joint and longitudinal joint UHPC pouring for the assembled guardrail segments: Firstly, pour UHPC in the area above the wing walls, covering up to the height of the concrete pavement layer (10 cm). Next, pour UHPC for the vertical connections inside the guardrail segments through the grouting ports reserved on the guardrail segments, as shown in Figs. 20e and f.

Table 3 compares the economic and social benefits of prefabricated segmental and cast-in-place monolithic guardrails. The prefabricated segmental guardrail has obvious advantages over the cast-in-place monolithic guardrail in terms of construction period, traffic interruption, Construction quality and social effects.

5 Conclusions

(1) Based on the results of the finite element simulation analyses of the crash processes of the three types of vehicles (cars, buses, and trucks), the UHPC-connected segmented prefabricated guardrails exhibited good blocking and guiding performances and better buffering and energy absorption effects than cast-in-place reinforced concrete guardrails.
(2) The crash test results on real vehicles verified that the key connection parts of UHPC are highly reliable and resistant to crash. In the crash test, the UHPC-con-

Table 3 Comparison of prefabricated segmental guardrail and cast-in-place monolithic guardrail

	Project	UHPC-Connected Prefabricated Segmental Guardrail	Cast-In-Place Monolithic Guardrail
1	Construction Period	7 Day	40 Day
2	Lane Closure Or Not	No	Yes
3	Construction Quality	Good Cosmetic Quality	Poor Cosmetic Quality
4	Construction Safety	Simple Process, Little Safety Hazard	Complex Process, Big Safety Hazard
5	Social Effects	Low Disruption And Impact On Local Communities During Construction	Adverse Effects Of Noise, Dust And Construction Debris On The Surrounding Environment During The Construction Period

nected segmented prefabricated guardrails exhibited good blocking, buffering, and guiding capabilities.

(3) Through practical engineering application, it is shown that prefabricated segmental guardrail has obvious advantages over the cast-in-place monolithic guardrail in terms of construction period, traffic interruption, Construction quality and social effects with good economic and social benefits, so it can be used as a reference for similar renovation projects.

Authors' contributions
Yinggen Li: Conceptualization, Investigation, Methodology, Writing—original draft. Zhiyong Li: Supervision, Resources, Methodology, Writing—review. Zheng Luo: Methodology, Writing—review. Nan Yu: Resources, Methodology, Writing—Review.

Funding
This work was supported by the Ningbo Natural Science Foundation (grant number 2023S178), Ningbo Transportation Science and Technology Project (grant number 202302.

Availability of data and materials
Presented in the main paper.

Declarations

Ethics approval and consent to participate
Not applicable.

Consent for publication
Not applicable.

Competing interests
Yinggen Li, Zhiyong Li, Zheng Luo, Nan Yu: No competing financial and non-financial interests in this paper.

Received: 12 January 2024 Accepted: 30 June 2024
Published online: 01 September 2024

References

Bandelt MJ, Adams MP, Wang H, Najm H, Bechtel A, Shirkorshidi SM, et al (2023) Advanced Reinforced Concrete Materials for Transportation Infrastructure: Final Report. In: New JIOT, The CONJ, Rutgers U, editors
Basit S, Maki T, Mutsuyoshi H, Ishihara Y, Tajima H (2020) Influence of reinforcement arrangement details on mechanical behavior of precast concrete barrier with loop connection. Structures. 27:1682–92
Charron JP, Niamba E, Massicotte B (2011) Static and Dynamic Behavior of High- and Ultrahigh-Performance Fiber-Reinforced Concrete Precast Bridge Parapets. J Bridge EnG. 16:413–21
Chen L, Wu H, Fang Q, Zhang T (2018) Numerical analysis of collision between a tractor-trailer and bridge pier. Int J Prot Struct. 9:484–503
Fan J, Shirkhorshidi SM, Adams MP, Bandelt MJ (2022) Predicting corrosion in reinforced UHPC members through time-dependent multi-physics numerical simulation. Constr Build Mater. 340:127805
Fan J, Adams M, Bandelt M (2023) "Service Life Prediction of RC and UHPC Bridge Decks Exposed to Regional Environments". International Interactive Symposium on Ultra-High Performance Concrete 3(1):29. https://doi.org/10.21838/uhpc.16656
Fang Z, Jiang H, Liu A, Feng J, Li Y (2020) Shear-friction behaviour on smooth interface between high-strength and lightweight concrete. Mag Concrete Res. 72:68–87
Gendron F, Desmettre C, Charron J (2022) Structural Behavior of Novel Precast TL-5 Bridge Barriers Using Ultrahigh-Performance Fiber-Reinforced Concretes. J Bridge Eng. 27:4021113
Hung C, El-Tawil S, Chao S (2021) A Review of Developments and Challenges for UHPC in Structural Engineering: Behavior, Analysis, and Design. J Struct Eng (United States) 1473121001
JTG B05-01 (2013) Standard for Safety Performance Evaluation of Highway Barriers. Ministry of Transport of the People's Republic of China, China
Khodayari A, Mantawy IM, Azizinamini A (2023) Experimental and Numerical Investigation of Prefabricated Concrete Barrier Systems Using Ultra-High-Performance Concrete Transport Res Rec J Transport Res Board. 2677:624–34
Liu C, Itoh Y, Kusama R (2007) Modeling and Simulation of Collisions of Heavy Trucks with Concrete Barriers. J Transport Eng. 133462–8
LSTC (2014) Livermore Software Technology Corporation. LS-DYNA keyword user's manual

Murray YD (2007) User's manual for LS-DYNA concrete material model 159. United States. Federal Highway Administration. Office of Research, Development, and Technology
Namy M, Charron J, Massicotte B (2015) Structural Behavior of Bridge Decks with Cast-in-Place and Precast Concrete Barriers: Numerical Modeling. J Bridge Eng. 20:4015014
Namy M, Charron J, Massicotte B (2015) Structural behavior of cast-in-place and precast concrete barriers subjected to transverse static loading and anchored to bridge deck overhangs. Can J Civil Eng. 42:120–9
Patel G, Sennah K, Azimi H, Lam C, Kianoush R (2014) Development of a precast concrete barrier wall system for bridge decks. PCI J. 59:83–102
Jeon SJ, Choi MS, Kim YJ (2011) "Failure mode and ultimate strength of precast concrete barrier." ACI Struct J 108(1):99
Shao Y, Nguyen W, Bandelt MJ, Ostertag CP, Billington SL (2022) Seismic Performance of High-Performance Fiber-Reinforced Cement-Based Composite Structural Members: A Review. J Struct Eng. 148:3122004
Sohail MG, Kahraman R, Al Nuaimi N, Gencturk B, Alnahhal W (2021) Durability characteristics of high and ultra-high performance concretes. J Build Eng. 33:101669
Yang J, Xu G, Cai CS, Kareem A (2019) Crash performance evaluation of a new movable median guardrail on highways. Eng Struct. 182:459–72

Publisher's Note